Polymer 51 (2010) 2548–2555

Contents lists available at ScienceDirect

Polymer

journal homepage: www.elsevier.com/locate/polymer

# Synthesis and characterization of a novel graft copolymer with poly(*n*-octylallene-*co*-styrene) backbone and poly(ε-caprolactone) side chain

Xufeng Ni*, Weiwei Zhu, Zhiquan Shen*

*MOE Key Laboratory of Macromolecular Synthesis and Functionalization, Department of Polymer Science and Engineering, Zhejiang University, Hangzhou 310027, People's Republic of China*

ARTICLE INFO

*Article history:*
Received 23 October 2009
Received in revised form
28 March 2010
Accepted 9 April 2010
Available online 24 April 2010

*Keywords:*
*n*-Octylallene
Copolymerization
Thiol-ene reaction

ABSTRACT

A novel graft copolymer consisting of poly(*n*-octylallene-*co*-styrene) (PALST) as backbone and poly(ε-caprolactone) (PCL) as side chains was synthesized with the combination of coordination copolymerization of *n*-octylallene and styrene and the ring-opening polymerization (ROP) of ε-caprolactone. Poly(*n*-octylallene-*co*-styrene) (PALST) backbone was prepared from the copolymerization of *n*-octylallene and styrene with high yield by using the coordination catalyst system composed of bis[N,N-(3,5-di-tert-butylsalicylidene)anilinato]titanium(IV) dichloride ($Ti(Salen)_2Cl_2$) and tri-isobutyl aluminum($Al(i\text{-}Bu)_3$). The molar ratio of each segment in the copolymer, and the molecular weight of the copolymer as well as the microstructure of the copolymer could be adjusted by varying the feeding ratio of both styrene and *n*-octylallene. The hydroxyl functionalized copolymer PALST–OH was prepared by the reaction of mercaptoethanol with the pendant double bond of PALST in the presence of radical initiator azobisisbutyronitrile (AIBN). The target graft copolymer [poly(*n*-octylallene-*co*-styrene)-*g*-polycaprolactone] (PALST-*g*-PCL) was synthesized through a grafting-from strategy via the ring-opening polymerization using PALST–OH as macroinitiator and $Sn(Oct)_2$ as catalyst. Structures of resulting copolymer were characterized by means of gel permeation chromatography (GPC) with multi-angle laser light scattering (MALLS), $^{13}C$ NMR, $^{1}H$ NMR, DSC, polarized optical microscope (POM) and contact angle measurements.



## 1. Introduction

Allene derivatives are attractive monomers because they have cumulated double bonds, which can be regarded as the isomers of propargyl derivatives. Allene derivatives are good candidates to produce reactive polymers bearing exomethylene substituents attached to the polymer backbone or those having internal double bonds in the main chain by the polymerization of either part (1,2- or 2,3-polymerization) of the cumulated double bonds [1]. Moreover, allene derivatives can also be used as attractive synthetic precursors for synthesizing functional materials due to the versatility of the addition reactions of the double bonds.

Allene derivatives can be polymerized with different polymerization mechanisms including radical, cationic, coordination and zwitterionic polymerization [1]. Endo and co-workers developed the living coordination polymerization of allene derivatives by π-allylnickel catalysts [2–7]. More recently, the living coordination polymerization of an allene monomer having homochiral binaphthyl and phenylcarbamoyloxy moieties was performed by $[(\pi\text{-ally})NiOCOCF_3]_2/PPh_3$ catalyst, yielding a polymer with a single-handed helical conformation in aprotic solvents [8]. The living coordination polymerization of allene derivatives in protic solvents can accelerate the polymerization and increase 1,2-polymerization selectivity [9]. Due to the stability of the living π-allylnickel ends of the polymers, the block copolymerizations of different allene derivatives [10,11], and allene derivatives with isonitrile [12] or isocyanides [13] proceed in a two-stage coordination polymerization process. However, the polymerizations of common vinyl monomers such as styrene and acrylate cannot be initiated by π-allylnickel catalysts, and consequently the copolymerization of allene derivatives with common vinyl monomers was not reported till now. Huang et al [14–16] synthesized graft copolymers with a polyallene-based backbone and poly(acrylate) side chains by the combination of π-allylnickel catalyzed living coordination polymerization of 6-methyl-1,2-heptadien-4-ol and atom transfer radical polymerization (ATRP) of methyl methacrylate or *tert*-butyl acrylate. Huang et al. also synthesized a new double bond based amphiphilic graft copolymer containing hydrophilic PEG side chains via coupling reaction between the

* Corresponding authors. Tel.: +86 571 879 53739; fax: +86 571 879 53727.
*E-mail addresses:* xufengni@zju.edu.cn (X. Ni), zhiquan_shen@163.com (Z. Shen).

0032-3861/$ – see front matter © 2010 Elsevier Ltd. All rights reserved.
doi:10.1016/j.polymer.2010.04.013

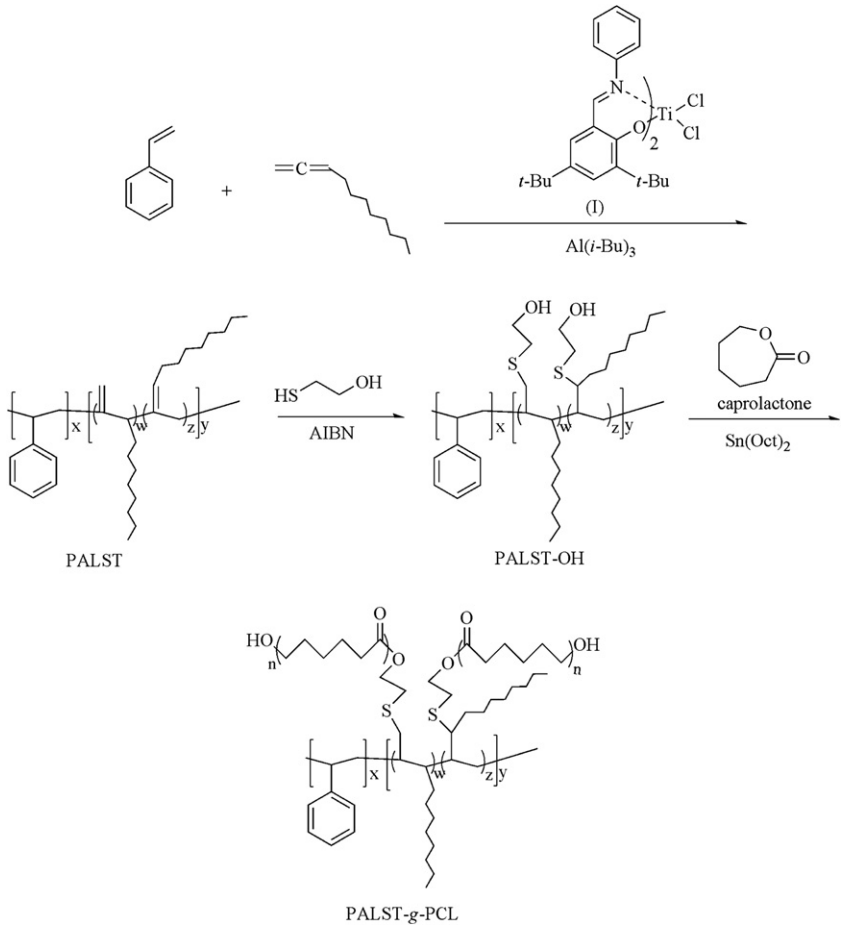


**Scheme 1.** Synthesis of novel graft copolymer PALST-*g*-PCL.

pendant hydroxyls of 6-methyl-1,2-heptadien-4-ol homopolymer and acyl chloride end group of functionalized MPEG using 4-dimethylamino as catalyzer [17]. Copolymers are of importance as materials whose functions are difficult to attain by any homopolymer systems [18]. The polymerization of vinyl-end monomers are quite useful methods for the designed synthesis of graft copolymers [19,20]. Allene moieties might be attractive polymerizable groups in terms of the improvement of the polymerizability and reactivity of the resulting double bond containing polymers. However, only the hydrosilylation and the oxidation reaction of polymers having polyallene units were reported [12,21].

**Table 1**
Copolymerization of *n*-Octylallene(A) and Styrene(St).[a]

| Run | [A]/[Ti] | [St]/[Ti] | $M_w$[b] ($10^4$) | $M_w/M_n$[b] | Yield (%) | Composition of copolymer | |
|---|---|---|---|---|---|---|---|
| | | | | | | A:St[c] | unit ratio(%)[d] |
| 1 | 100 | 100 | 1.69 | 1.58 | 100 | 47:53 | 37:63 |
| 2 | 100 | 200 | 2.61 | 1.61 | 100 | 34:66 | 31:69 |
| 3 | 100 | 500 | 3.14 | 1.63 | 86 | 24:76 | 21:79 |
| 4 | 100 | 1000 | 5.24 | 1.64 | 85 | 22:78 | 14:86 |
| 5 | 100 | 1500 | 8.13 | 1.68 | 87 | 14:86 | 12:88 |
| 6 | – | 400 | – | – | <1 | – | – |
| 7 | 50 | 350 | 4.61 | 1.72 | 100 | 15:85 | 12:88 |
| 8 | 100 | 300 | 3.81 | 1.76 | 100 | 28:72 | 17:83 |
| 9 | 150 | 250 | 2.87 | 1.49 | 100 | 35:65 | 22:78 |
| 10 | 200 | 200 | 1.80 | 1.58 | 100 | 50:50 | 36:64 |
| 11 | 250 | 150 | 1.27 | 1.49 | 100 | 66:34 | 42:58 |
| 12 | 300 | 100 | 1.21 | 1.66 | 100 | 74:26 | 54:46 |

[a] Polymerization conditions: [Al]/[Ti] = 50, aged at 80 °C for 3h, polymerized at 80 °C for 16h in bulk.
[b] Determined by GPC against the standard PSt samples.
[c] The molar ratio of two segments determined by $^1$H NMR.
[d] The molar ratio of 1,2-polymerized units(w) and 2,3-polymerized units(z) of the poly(*n*-octylallene) moieties in the main chain, determined by $^1$H NMR.

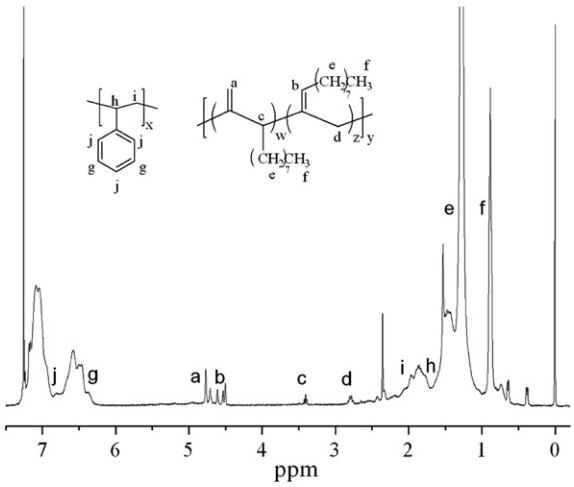


**Fig. 1.** $^1$H NMR spectrum of PALST (Run 1 in Table 1).

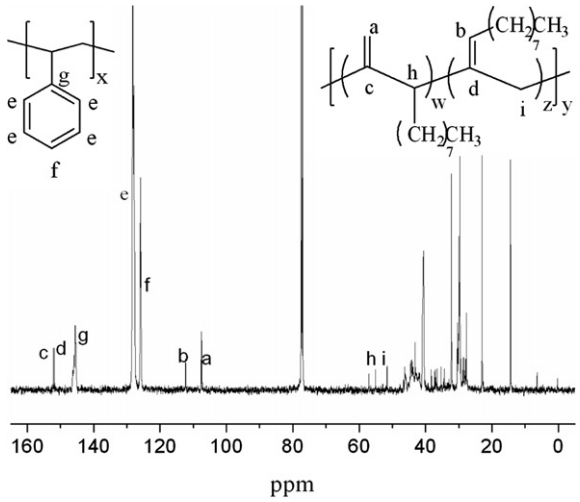


**Fig. 2.** $^{13}C$ NMR spectrum of PALST (Run 1 in Table 1).

Thiol-ene chemistry has recently been shown to be a valuable synthetic tool, particularly in the area of materials chemistry [22–25]. Thiol-ene reactions involve the sulfur version of the hydrosilylation reaction and the addition of a sulfur-hydrogen bond across a double or triple bond. Depending on the reaction conditions and the unsaturated substrates, the thiol-ene reaction can proceed by either a free radical or an ionic mechanism. The advantage of the thiol-ene reaction is apparent: moisture and air do not need to be excluded, expensive transition metal catalysts are unnecessary, a wide variety of functional groups and solvents (including water) are tolerated, and high yields and clean products are obtained [25–28].

Previously, we have reported the polymerization of *n*-octylallene with the coordination catalyst system composed of bis[N, N-(3,5-di-tert-butylsalicylidene) anilinato] titanium(IV) dichloride ($Ti(Salen)_2Cl_2$) and tri-isobutyl aluminum ($Al(i\text{-}Bu)_3$) [29]. In this paper, the same catalytic system is used for the copolymerization of *n*-octylallene and styrene, the copolymer (PALST) obtained was functionalized with hydroxyl group by the thiol-ene reaction between mercaptoethanol and PALST to provide the modified copolymer PALST–OH. The graft copolymer [poly(*n*-octylallene-*co*-styrene)-*g*-poly(ϵ-caprolactone)] (PALST-*g*-PCL) was synthesized using PALST–OH as macroinitiator via the controlled ring-opening polymerization of ϵ-caprolactone (Scheme 1).

## 2. Experimental

### 2.1. Materials and measurements

Bis[N,N-(3,5-di-*tert*-butylsalicylidene)anilinato]titanium(IV) dichloride and *n*-octylallene (A) were prepared as previously reported [29]. Tetrahydrofuran (THF), toluene, diethyl ether were dried over sodium and distilled under nitrogen. ϵ-caprolactone (CL Acros 99%) and styrene (St) (Shanghai chemical reagent company) were distilled over $CaH_2$ under reduced pressure prior to use. 2,2′-azobis(2- methylpropanenitrile) (AIBN) was purified by recrystallization from methanol. Other reagents were used as received.

$^{13}C$ NMR and $^{1}H$ NMR spectra were recorded on a Bruker Avance DMX500 spectrometer (500 MHz) using $CDCl_3$ as solvent at 25 °C with TMS as internal reference. Gel permeation chromatography (GPC) with UV (Waters 2487) and RI (Waters 2414) detection system equipped with a Waters 1525 isocratic high performance liquid chromatography pump, was carried out at 40 °C with THF as the eluent at a flow rate of 1.0 mL/min against the standard polystyrene samples. Multi-Angle Laser Light Scattering (MALLS) measurement was obtained at 40 °C on a setup including a Waters 510 pump, a Wyatt DAWN DSP multi-angle light scattering photometer and a Wyatt OPTILAB DSP interferometric refractometer. FT-IR spectra were recorded on a Bruker Vector 22 FT-IR spectrometer using KBr pellet, the samples were prepared by casting one drop of a chloroform solution containing 10 wt.% copolymer on a clean KBr pellet and then airing for 1h followed by drying under vacuum for 3h at room temperature. Contact angle measurement was using a contact angle meter (OCA 20, Datapysics Instruments GmbH Germany) at 25 °C and at about 65% relative humidity. Differential scanning calorimetry (DSC) curves were carried on a DSC TA Q100 thermal analysis system (Shimadzu, Japan), the samples were heated from −20 °C to 100 °C (first heating run), held for 3 min to erase the thermal history, then cooled to −20 °C at a rate of 10 °C/min, and heated again to 100 °C (second heating run) at a rate of 10 °C/min. The morphology of samples was monitored with the polarized optical microscope (POM) (Olympus BX51) equipped with a heating stage (Linksys css450), the samples were prepared by casting three drops of a chloroform solution containing 0.5 wt.% copolymer on a clean cover glass and then airing for 1 day at room temperature followed by drying under vacuum for 1 day.

### 2.2. Copolymerization of n-octylallene and styrene

All polymerizations were performed in 25 mL ampoules under argon atmosphere using Schlenk techniques. In a typical

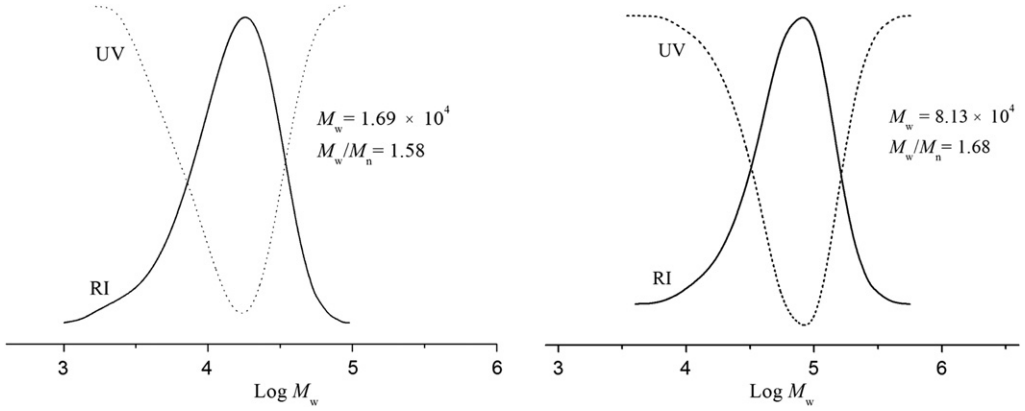


**Fig. 3.** GPC traces of a copolymer of Run 1 (a) and Run 5 (b) by RI and UV detectors.

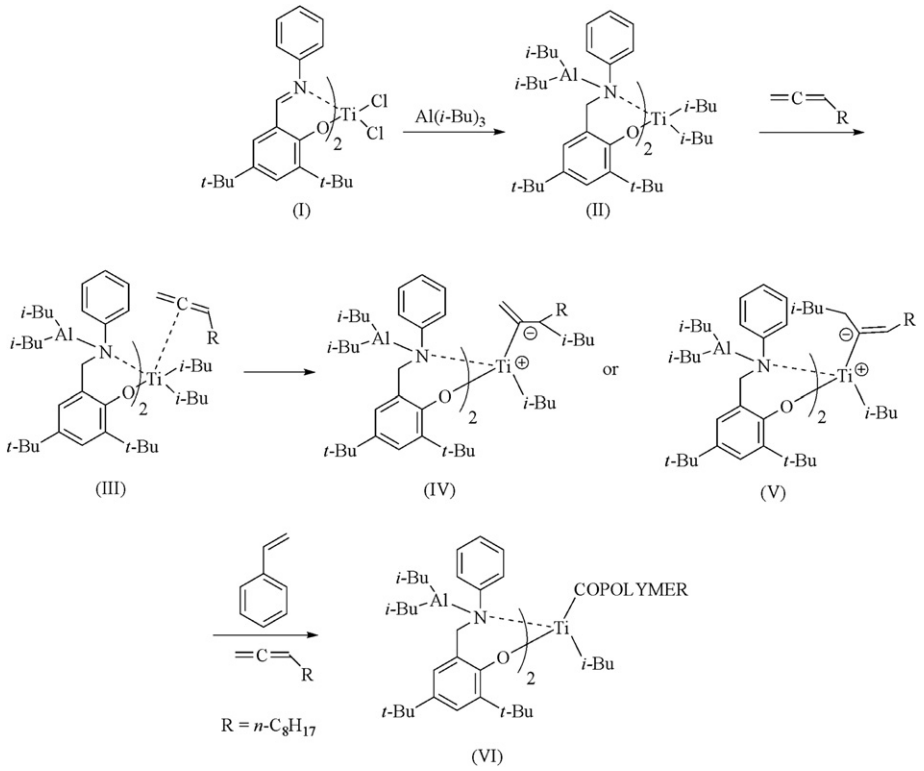


**Scheme 2.** Possible mechanism of the copolymerization.

copolymerization, 0.05g (0.07 mmol) catalyst $Ti(Salen)_2Cl_2$ was transmitted into the ampoule, then the cocatalyst $Al(i\text{-}Bu)_3$ was injected by syringe, and the mixture was aged for a certain period. Monomers (*n*-octylallene and styrene) were introduced into the ampoule, and the polymerization was carried out under the certain polymerization conditions. The polymerization was terminated and precipitated by methanol with 5% HCl, and washed with methanol several times, dried in vacuum at room temperature for 24h. The compositions of the resulting copolymers were determined from $^1$H NMR spectra by comparing the integrals of the signals of aromatic protons at 6.3–7.1 ppm and those side chains of poly (*n*-octylallene) at 0.9 ppm ($-CH_3$) and 1.4 ppm ($-(CH_2)_7-CH_3$).

### 2.3. Thiol based functionalization of the copolymer PALST

An efficient approach for a one-step modification of polymer precursors is the free-radical addition of ω-functional mercaptans [30,31] onto vinyl double bonds. The former reaction has also been used for an end-functionalization of polymers [32]. In our case, mercaptoethanol (RSH) and AIBN with a molar ratio of $[RSH]_0/[C{=}C]_0/[AIBN]_0 = 40:1:0.33$ were added into a toluene solution of PALST (~3 wt.%), the excess mercaptoethanol was used to make the reaction complete. The mixture reacted at 70 °C for 24h under a dry nitrogen atmosphere. The crude product was precipitated several times in MeOH, washed with water and dried under vacuum to constant weight.

### 2.4. Preparation of PALST-g-PCL through PALST–OH

The grafting-from [33] strategy was employed to synthesize the graft copolymers of PALST and CL via ring-opening polymerization

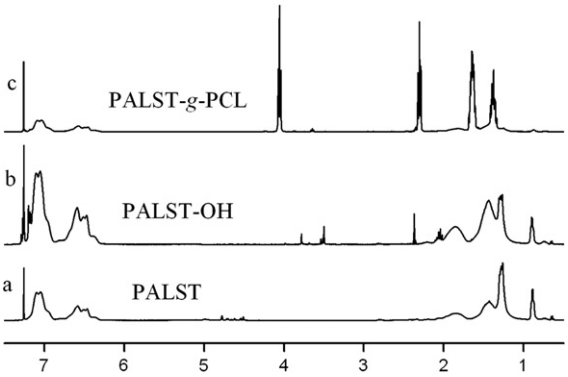


**Fig. 4.** $^1$H NMR spectra of PALST(Run 8 in Table 1), PALST–OH and $PALST_a$-*g*-$PCL_{10}$.

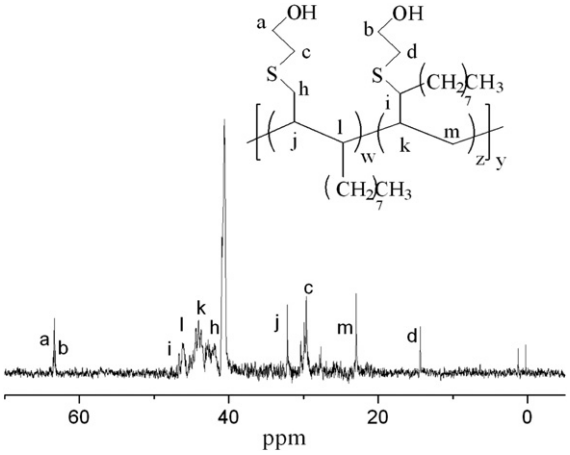


**Fig. 5.** $^{13}$C NMR spectrum of PALST–OH.

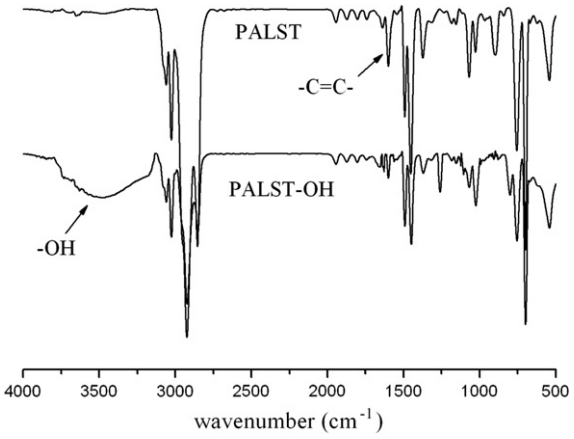


**Fig. 6.** FT-IR spectra of PALST (Run 8 in Table 1) and PALST–OH.

of CL using PALST–OH as macroinitiator. PALST–OH was dissolved with CL in a dry flask, evacuated and backfilled with nitrogen for several times, $Sn(Oct)_2$ was added to the solution under nitrogen atmosphere, and the flask was heated at 100 °C for 4 h. The resulting clear, viscous mixture was cooled to room temperature and dissolved in toluene, and the product was precipitated and washed by methanol several times, dried under vacuum to constant weight.

## 3. Results and discussion

### 3.1. Features of copolymerization of n-octylallene and styrene

The copolymerization of allene derivatives with common vinyl monomers was not reported. We have reported that $Ti(Salen)_2Cl_2$/$Al(i\text{-}Bu)_3$ catalytic system is an effective catalyst for the homopolymerization of *n*-octylallene [29], but could hardly homopolymerize styrene. However, the copolymerization of styrene with *n*-octylallene can carry out using this catalytic system as shown in Table 1. For example, the coordination copolymerization of styrene and *n*-octylallene (Run 1 in Table 1) was carried out under the following conditions: [A]/[St]/[Ti] = 100/100/1, [Al]/[Ti] = 50, copolymerized at 80 °C for 16h, giving the copolymer in 100% yield, with $M_w = 1.69 \times 10^4$ and $M_w/M_n = 1.58$. The $M_w$ of the copolymer increased with increasing styrene ratio, while the yields fairly decreased to around 85%. From the $^1H$ NMR spectrum of the copolymer (Fig. 1), the molar ratio of styrene and *n*-octylallene

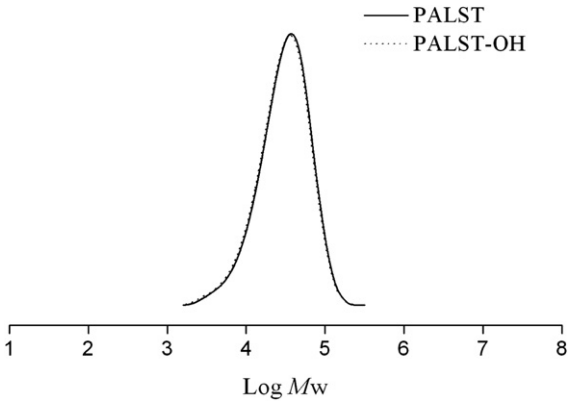


**Fig. 7.** GPC traces of copolymer PALST (Run 8 in Table 1) and PALST–OH by RI detectorf.

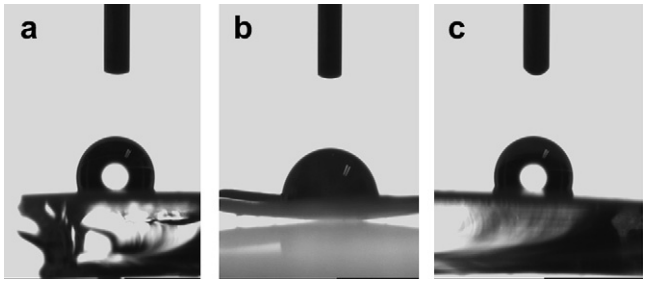


**Fig. 8.** Contact angle of copolymers [PALST(a, Run 8 in Table 1), PALST–OH(b) and $PALST_a$-g-$PCL_{10}$(c)].

segments (labeled x and y in Scheme 1) was determined to be 53:47, close to the feeding ratio (50:50). Fig. 1 also shows that the copolymer PALST consists of both 1,2- and 2,3-polymerized *n*-octylallene units (labeled w and z respectively in Scheme 1). The molar ratio of the two units (w:z) is 37:63, which was determined by integration of $^1H$ NMR signals at 4.7–5.2 ppm as described in reference [2]. $^{13}C$ NMR spectrum (Fig. 2) confirms the structure of the copolymer.

GPC curves of the copolymers (Run 1 and Run 5 in Table 1) are shown in Fig. 3, the peaks have unimodal distribution. Moreover, elution peaks of both RI and UV($\lambda$ = 254 nm) detectors were harmony with each other, indicating that the copolymer obtained did not contain either homopolymer [34].

The copolymerizations of styrene and *n*-octylallene were also investigated under a fixed total monomer concentration [St + A]/[Ti] = 400 (molar ratio) with varying feeding ratios of two monomers (Run 7–12, Table 1). Despite of the variety of monomer feeding ratio, the copolymer yields always reached 100%. The molar ratio of two segments in the copolymer is close to their feeding ratio. Molecular weights of the copolymers increased with the increasing of styrene ratio, and the proportion of 1,2- to 2,3-polymerzation units increased with the decreasing of styrene segments in the copolymer chain. From these results, it can be concluded that the length of each segment in the copolymer, and the molecular weight of the copolymer as well as the microstructure of the copolymer could be adjusted by varying the feeding ratio of styrene and *n*-octylallene.

Neither $Ti(Salen)_2Cl_2$ nor $Al(i\text{-}Bu)_3$ alone can catalyze the copolymerization of *n*-octylallene and styrene. Possible monomer insertion mechanism is illustrated in Scheme 2. $Ti(Salen)_2Cl_2$ reacts with $Al(i\text{-}Bu)_3$ generated a phenoxyamine complex as the catalytically active species (II in Scheme 2) as reported [35–37]. Considering this amine nitrogen with an alkylaluminum group is a weak

**Table 2**
Graft copolymerization of ϵ-caprolactone on PALST backbone.[a]

| Samples | DP of PCL | | GPC[d] | | MALLS[e] | |
|---|---|---|---|---|---|---|
| | Feed[b] | Exp.[c] | $M_w(10^4)$ | MWD | $M_w(10^4)$ | MWD |
| $PALST_a$[f] | | – | 3.81 | 1.76 | 2.57 | 1.72 |
| $PALST_a$-g-PCL10 | 10 | 8.0 | 3.74 | 1.82 | 3.63 | 1.53 |
| $PALST_b$[g] | | – | 5.24 | 1.64 | 3.21 | 1.68 |
| $PALST_b$-g-PCL25 | 25 | 21.4 | 5.20 | 1.72 | 4.33 | 1.41 |
| $PALST_b$-g-PCL40 | 40 | 44.5 | 5.83 | 1.73 | 6.74 | 1.52 |

[a] Polymerization conditions: Polymerized at 110 °C for 4h in bulk.
[b] CL feeding ratio ([CL]/[OH]).
[c] Experimental results determined by $^1H$ NMR in $CDCl_3$.
[d] Determined by GPC against the standard PSt samples connecting RI and UV detectors.
[e] Determined by GPC equipped with a MALLS detector.
[f] Run 8 in Table 1.
[g] Run 4 in Table 1.

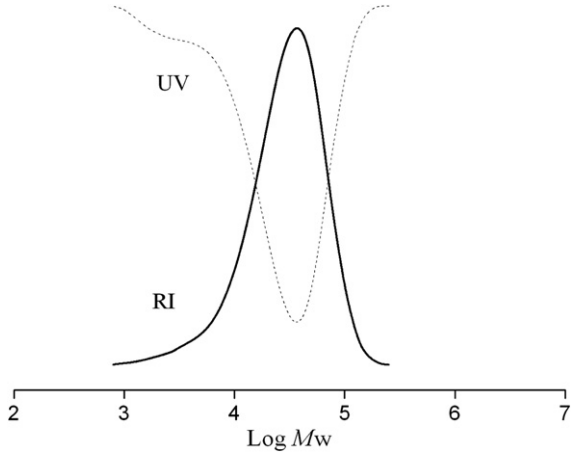


**Fig. 9.** GPC traces of the copolymer $PALST_a$-g-PCL10.

donor, and provides a weak N–Ti interaction and the phenoxy-amine complex potentially possesses higher electrophilicity at the Ti center. Thus, intermediate II can not catalyze the homopolymerization of styrene. When *n*-octylallene existed, *n*-octylallene would coordinate on the central Ti atom to form the intermediate III similar to the case of other transition metals [1,38]. The insertion of *n*-octylallene might produce a vinyl anion as IV or V, which could be an active center and very likely to be able to polymerize styrene. Thus, the sequence insertion of styrene in this copolymerization was feasible to produce the corresponding copolymers.

### 3.2. Modification of the double bond on the copolymer PALST

The PALST copolymers prepared have unsaturated exo-methylenes structure, and could react with thiol based substances. Mercaptoethanol was introduced to react with the pendant double bond of PALST so that the hydroxyl group was introduced onto PALST (referred to as PALST–OH). Structure of PALST–OH was confirmed by $^1$H NMR, $^{13}$C NMR, FT-IR and GPC measurements (Figs. 4–7). In $^1$H NMR spectrum (Fig. 4), there is no signal at $\delta$ = 4.7–5.2 ppm and new thioether linkages (—$CH_2SCH_2$—) at 2.6–2.8 ppm appear [39]. The detailed information of the micro-structural units in PALST–OH could be obtained by its $^{13}$C NMR analysis (Fig. 5). That is, new signals for –CH(–*C*H(SR)($C_8H_{17}$))— and –CH(–*C*$H_2$SR)— were observed at 46.7 ppm and 41.1 ppm, besides the signals at 62.4 ppm and 63.1 ppm attributable to –*C*–OH. Meanwhile, signals of –*C*(SR)(–$CH_2$($C_8H_{17}$))— and –*C*H(SR)(–$CH_3$)— were not found, indicating that this thiol addition reaction proceeds with anti-Markownikoff orientation, which consists with the references [40,41]. The FT-IR spectra of PALST and PALST–OH (Fig. 6) show the characteristic absorption of double bonds at 1640 cm$^{-1}$ (PALST) or declined (PALST–OH). The lack of –SH resonances at around 2550–2600 cm$^{-1}$ indicates that ether groups are indeed covalently attached to the polymer backbone and that the products are free of mercaptan impurities. On the other hand, the characteristic resonance signal of –OH around 3250–3500 cm$^{-1}$ (PALST–OH) confirmed that the thiol addition reaction was complete. GPC measurement shows that there is no obvious difference of molecular weight and molecular weight distribution between PALST and PALST–OH (Fig. 7).

Surface contact angle of PALST and PALST–OH are shown in Fig. 8, it is found that the average contact angle of the copolymer was reduced from 106.3° (Fig. 8a PALST) to 81.9° (Fig. 8b PALST–OH) after the mercaptoethanol addition, indicating that the hydroxyl groups have been introduced into the PALST backbone.

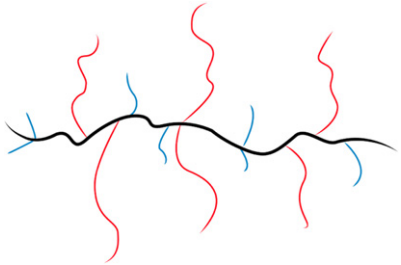

**Scheme 3.** The assumption morphology of the PALST-g-PCL.

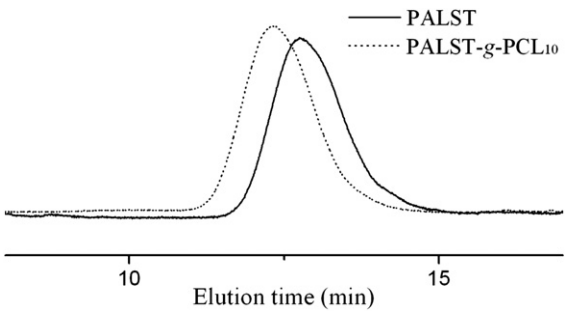


**Fig. 10.** MALLS/GPC traces of the copolymers in Table 2.

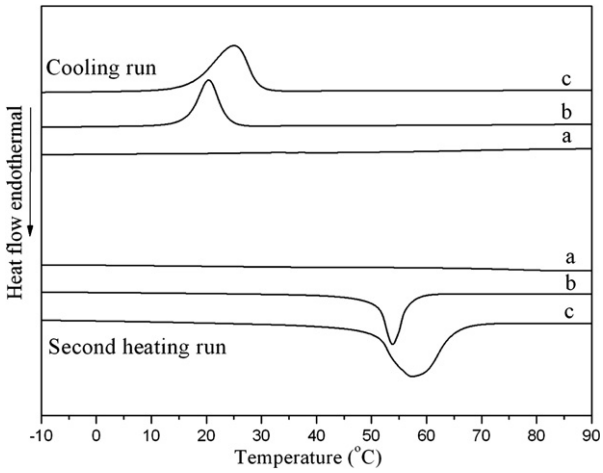


**Fig. 11.** DSC curves of (a) $PALST_a$-g-$PCL_{10}$ (b) $PALST_b$-g-$PCL_{25}$ (c) $PALST_b$-g-$PCL_{40}$ in the cooling run and the second heating run, respectively.

**Table 3**
Thermal behaviors of PALST-g-PCL determined by DSC.

| Samples | $T_c$(°C)[a] | $T_m$(°C)[b] | $\Delta H_m$(J/g)[c] | $X_c$(%)[d] |
|---|---|---|---|---|
| $PALST_a$-g-PCL10 | – | – | – | – |
| $PALST_b$-g-PCL25 | 20.1 | 53.6 | 46.4 | 34.1 |
| $PALST_b$-g-PCL40 | 24.9 | 56.8 | 69.9 | 51.4 |

[a] $T_c$ denotes the crystallization temperatures in the cooling run.
[b] $T_m$ is the melting point in the second heating run.
[c] $\Delta H_m$ denotes the fusion in the second heating run.
[d] $X_c = \Delta H_m/\Delta H^0_{m,PCL}$, where $\Delta H^0_{m,PCL}$ is 136.1 J/g.

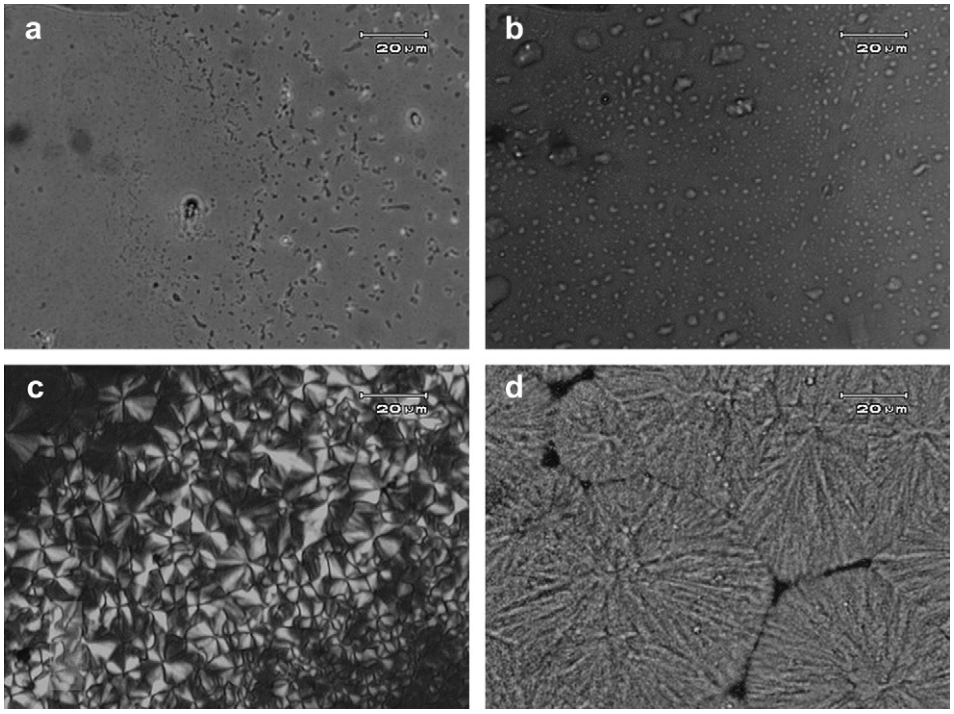


**Fig. 12.** POM micrographs of spherulites of PALST-*g*-PCL isothermal crystallized at 30 °C for about 20min.(a) $PALST_b$ (b) $PALST_a$-*g*-$PCL_{10}$ (c) $PALST_b$-*g*-$PCL_{25}$ (d) $PALST_b$-*g*-$PCL_{40}$.

### 3.3. *Synthesis and characterization of PALST-g-PCL graft copolymer*

The graft copolymerization of ϵ-caprolactone on PALST backbone was carried out in bulk using PALST–OH as macroinitiator and stannous octoate as catalyst, and the results are listed in Table 2. The feeding molar ratio of CL and hydroxyl groups of PALST–OH was varied ([CL]/[OH] = 10, 25, and 40), assumes that every hydroxyl group of PALST–OH chains took part in initiation. The yield of all the ring-opening graft copolymerizations achieved 100%. From the $^1$H NMR spectrum, signals originated from all units (*n*-octylallene, styrene and CL) are detected (Fig. 4c). Contact angle measurement (Fig. 8c) shows that the hydrophilicity of PALST-*g*-PCL was reduced as compared with that of PALST–OH. Fig. 9 shows the GPC curves of $PALST_a$-*g*-$PCL_{10}$ using RI and UV detector, all of the two GPC traces show unimodal, and have same molecular weight or molecular weight distribution, indicating there was no any PCL homopolymer and unreacted PALST–OH. These characterizations demonstrate that graft copolymer has been prepared.

The molecular weights of all the copolymers determined by GPC using RI and UV detectors show no remarkable change with CL units grafted (Table 2). This is reasonable for copolymer seems to have the cylindrical brush morphology (Scheme 3) [42–44]. In order to confirm the influence of CL units on $M_w$ of the graft copolymer, GPC coupled with multi-angle laser light scattering (MALLS) detector was used, and the results are shown in Fig. 10 and Table 2. The MALLS/GPC traces shifts to the higher molar masses region along with disappearance of the peak of the precursor. These chromatograms unambiguously show the formation of the PCL proportion on the copolymer chain.

The thermal behaviors of PALST-*g*-PCL graft copolymers were investigated by DSC as shown in Fig. 11 and Table 3. The crystallization temperature ($T_c$) was obtained from the cooling run, and the melting temperature ($T_m$) and the degree of crystallinity ($X_c$) was obtained from the second heating run. The results listed in Table 3 show that $T_c$, $T_m$ and $X_c$ of PALST-*g*-PCL increase with the increasing length of grafted PCL chains.

Fig. 12 shows the POM micrographs of the graft copolymers with various PCL lengths isothermally crystallized at 30 °C. The PCL segments with less length had low crystallization ability, as illustrated in Fig. 12. Graft copolymers with longer PCL have crystal clearly (Fig. 12c, d). POM micrographs match the data of DSC analysis quite well, indicated that the intricate structure of the graft copolymer resulted in decreasing the crystallization ability of PCL segment.

## 4. Conclusions

A novel brush graft copolymer with a poly(*n*-octylallene-*co*-styrene) backbone and poly(ϵ-caprolactone) side chains was synthesized and characterized. The copolymer backbone was constructed by the coordination copolymerization of *n*-octylallene with styrene using $Ti(Salen)_2Cl_2/Al(i\text{-}Bu)_3$ catalytic system. Followed the transformation of the pendant double bond of PALST into PALST–OH, the target graft copolymer, PATSL-*g*-PCL was synthesized. The newly prepared graft copolymer was characterized by means of gel permeation chromatography (GPC) with multi-angle laser light scattering (MALLS), $^{13}$C NMR, $^1$H NMR, DSC, polarized optical microscope (POM) and contact angle measurements. The thermal and crystallization behavior of the PALST-*g*-PCL was also examined.

## Acknowledgements

The authors gratefully acknowledge the financial supports of the National Natural Science Foundation of China (G20874083, 20774078), and the Special Funds for Major Basic Research Projects (G2005CB623802).

## References

[1] Endo T, Tomita I. Prog Polym Sci 1997;22:565–600.
[2] Tomita I, Kondo Y, Takagi K, Endo T. Macromolecules 1994;27:4413–4.

[3] Takagi K, Tomita I, Nakamura Y, Endo T. Macromolecules 1998;31:2779–83.
[4] Takagi K, Tomita I, Endo T. Macromolecules 1997;30:7386–90.
[5] Takagi K, Tomita I, Endo T. Macromolecules 1998;31:6741–7.
[6] Taguchi M, Tomita I, Endo T. Angew Chem Int Ed 2000;39:3667–9.
[7] Takagi K, Tomita I, Endo T. Polym Bull 2003;50:335–42.
[8] Mochizuki K, Tomita I. Macromolecules 2006;39:6336–40.
[9] Kino T, Taguchi M, Tazawa A, Tomita I. Macromolecules 2006;39:7474–8.
[10] Takagi K, Tomita I, Endo T. Polym Bull 1997;39:685–92.
[11] Tomita I, Abe T, Takagi K, Endo T. J Polym Sci Part A Polym Chem 1995;33:2487–92.
[12] Taguchi M, Tomita I, Endo T. Macromol Chem Phys 2000;201:2322–7.
[13] Tomita I, Taguchi M, Takagi K, Endo T. J Polym Sci Part A Polym Chem 1997;35:431–7.
[14] Zhang XH, Peng D, Lu GL, Gu LN, Huang XY. J Polym Sci Part A Polym Chem 2006;44:6888–93.
[15] Zhang XH, Shen Z, Li LT, Lu GL, Gu LN, Huang XY. Polymer 2007;48:5507–13.
[16] Peng D, Zhang XH, Feng C, Lu GL, Zhang S, Huang XY. Polymer 2007;48:5250–8.
[17] Zhang XH, Shen Z, Feng C, Yang D, Li YG, Hu JH, et al. Macromolecules 2009;42:4249–56.
[18] Taguchi M, Tomita I, Yasuhiko Y, Endo T. J Polym Sci Part A Polym Chem 1999;37:3916–21.
[19] Ito K, Tsuchida H, Kitano T. Polym Bull 1986;15:425–30.
[20] Ito K, Yokoyama S, Arakawa F, Yukawa Y, Iwashita T, Yamasaki Y. Polym Bull 1986;16:337–44.
[21] Kino T, Tomita I. Polym Bull 2005;55:251–8.
[22] Campos LM, Meinel I, Guino RG, Schierhorn M, Gupta N, Stucky GD, et al. Adv Mater 2008;20:3728–33.
[23] Dondoni A. Angew Chem Int Ed 2008;47:8995–7.
[24] Li Q, Zhou H, Wicks DA, Hoyle CE. J Polym Sci Part A Polym Chem 2007;45:5103–11.
[25] Hoyle CE, Lee TY, Roper T. J Polym Sci Part A Polym Chem 2004;42:5301–38.
[26] Rissing C, Son DY. Organometallics 2008;27:5394–7.
[27] Rim C, Lahey LJ, Patel VG, Zhang HM, Son DY. Tetrahedron Lett 2009;50:745–7.
[28] Griesbaum K. Angew Chem Int Ed Engl 1970;9:273–87.
[29] Zhu WW, Ni XF, Shen ZQ. Chem J Chinese Universities 2008;29:2554–7.
[30] Serniuk GE, Banes FW, Swaney MW. J Am Chem Soc 1948;70:1804–8.
[31] Cunneen JI, Shipley FW. J Polym Sci 1959;36:77–90.
[32] Boileau S, Mazeaud-Henri B, Blackborow R. Eur Polym J 2003;39:1395–404.
[33] Zhang MF, Müller AHE. J Polym Sci Part A Polym Chem 2005;43:3461–81.
[34] Fodor Z, Fodor A, Kennedy JP. Polym Bull 1992;29:689–96.
[35] Saito J, Suzuki Y, Makio H, Tanaka H, Onda M, Fujita T. Macromolecules 2006;39:4023–31.
[36] Lamberti M, Consolmagno M, Mazzeo M, Pellecchia C. Macromol Rapid Commun 2005;26:1866–71.
[37] Saito J, Onda M, Matsui S, Mitani M, Furuyama R, Tanaka H, et al. Macromol Rapid Commun 2002;23:1118–23.
[38] Choi JC, Yamaguchi I, Osakada K, Yamamoto T. Macromolecules 1998;31:8731–6.
[39] Justynska J, Hordyjewicz Z, Schlaad H. Polymer 2005;46:12057–64.
[40] Gauthier MA, Gibson MI, Klok HA. Angew Chem Int Ed 2009;48:48–58.
[41] Justynska J, Schlaad H. Macromol Rapid Commun 2004;25:1478–81.
[42] Luo XL, Wang GW, Pang XC, Huang JL. Macromolecules 2008;41:2315–7.
[43] Li HY, Riva R, Jérôme R, Lecomte P. Macromolecules 2007;40:824–31.
[44] Li YX, Nothnagel J, Kissel T. Polymer 1997;38:6197–206.